

Can realistic interaction be useful for nuclear mean-field approaches?

H. Nakada¹, K. Sugiura¹, T. Inakura^{1,2,3}, and J. Margueron⁴

¹ Department of Physics, Graduate School of Science, Chiba University, Yayoi-cho 1-33, Inage, Chiba 263-8522, Japan

² Yukawa Institute of Theoretical Physics, Kyoto University, Kitashirakawa Oiwake-cho, Sakyo, Kyoto 606-8502, Japan

³ Department of Physics, Niigata University, Niigata 950-2181, Japan

⁴ Université de Lyon 1, CNRS/IN2P3, Institut de Physique Nucléaire de Lyon, F-69622 Villeurbanne, France

Received: date / Revised version: date

Abstract. Recent applications of the M3Y-type semi-realistic interaction to the nuclear mean-field approaches are presented: (i) Prediction of magic numbers and (ii) isotope shifts of nuclei with magic proton numbers. The results exemplify that realistic interaction, which is derived from the bare $2N$ and $3N$ interaction, furnishes a new theoretical instrument for advancing nuclear mean-field approaches.

PACS. 21.60.Jz Nuclear Density Functional Theory and extensions (includes Hartree-Fock and random-phase approximations) – 21.30.Fe Forces in hadronic systems and effective interactions – 21.10.Pc Single-particle levels and strength functions – 21.10.Ft Charge distribution

1 Introduction

Since atomic nuclei are self-bound systems, self-consistent approaches are of particular importance for the theoretical description of nuclear structure. The self-consistent mean-field (MF) or energy-density-functional (EDF) approaches, *i.e.* the Hartree-Fock (HF) and Hartree-Fock-Bogolyubov (HFB) approaches, are suitable for describing structure of nuclei in a wide range of the nuclear mass table. One of the great advantages of these approaches is the self-consistency between the one-body fields and the single-particle (s.p.) wave functions [1]. In nuclear physics, the self-consistent HF calculations were started by applying the zero-range Skyrme interaction [2,3]. While they have been successful, the nuclear interaction is known to be short but finite range. The self-consistent HFB calculations were first implemented by Daniel Gogny and his collaborators [4,5] with a finite-range interaction, the so-called Gogny interactions.

Since it is comprised only of contact terms, the HF energy derived from Skyrme-type interactions [6,7] is expressed in terms of the quasi-local EDF, *i.e.* by using only local currents including derivatives of the s.p. functions. Because of its computational simplicity originating from its quasi-local character, the Skyrme EDF has been most widely used in the self-consistent MF calculations. While the HF potential includes only the particle-hole (ph) channel of the effective interaction, the particle-particle (pp) channel defines the pairing properties and enters in the HFB equation. The Skyrme EDF was later extended to

include the pp channel. However, since a contact form of attraction is taken also for the pp channel, certain cutoff scheme is required to avoid divergence. The cutoff usually depends on the solution (*e.g.* the s.p. energies), and thereby violates the variational character even though its influence could be small. Moreover, the pp channel is assumed to be independent of the ph channel in the Skyrme EDF, except the SkP parameter-set [8]. It is shown that the microscopic effective interaction is different between the ph and the pp channels in infinite systems such as nuclear matter [9], because the s.p. space is separated between these channels. This may hold also in vicinity of doubly magic nuclei. In the density-functional theory (*e.g.* the Kohn-Sham theory), there is no need to assume underlying interaction, and thereby no relation between the ph and the pp channels. It is noted, however, that the s.p. functions in the Kohn-Sham theory are artifacts, losing their physical meaning. In the HFB calculations for finite open-shell nuclei, nucleons on certain orbitals can lie in the ph and the pp channels simultaneously. It will be natural that there is an interaction consistent for both channels in that case, and finite-range interactions offer the possibility to define a unique interaction for these channels.

Owing to the Gaussian form for the central force, the Gogny interaction is free of these problems. The central force of the original parameter-set D1 [5] was partially related to the Brueckner HF results in the nuclear matter. To some extent, it could be said that the D1 interaction has a nature not far from the realistic nuclear interaction. The connection to the realistic interaction was lost in the phenomenologically ‘modified’ parameter-sets that came

Send offprint requests to:

after such as D1S [10] and D1M [11]. For the non-central part of these forces, the contact interaction type is usually adopted. This is the case for the LS force, which is identical to the one of the Skyrme interaction. The tensor force has been ignored in the widely used parameter-sets of the Gogny interaction. Although several parameter-sets including the tensor force have been proposed [12,13,14], underlying the importance of the tensor force in the MF regime [15,16], their application has yet been limited.

One of the authors (H.N.) has developed another type of finite-range effective interaction applicable to the self-consistent MF calculations; the M3Y-type interaction [17, 18]. This may be categorized as *semi-realistic*. It is based on the M3Y interaction [19,20] that was derived from the G -matrix, and includes phenomenological modification so as to reproduce the saturation and ℓs splitting in finite nuclei. Because of its connection to the realistic interaction, the M3Y-type interaction will be suitable to address the question raised as the title of this paper. In this paper we shall mainly present results using the M3Y-P6 parameter-set and its variant, particularly focusing on the non-central forces. M3Y-P n with $n \geq 5$, including M3Y-P6, contains a tensor force that is the same as the one contained in the M3Y-Paris interaction [20]. This enables us to study roles of the tensor force on a realistic basis. An overall factor is applied to the LS force in order to obtain reasonable s.p. level sequence in ^{208}Pb . For this part, a variant of M3Y-P6 has been introduced in Ref. [21], motivated by the recent finding related to the three-nucleon ($3N$) interaction. This new interaction reinforces the link to the realistic interaction.

2 M3Y-type interaction and mean-field calculations

The effective Hamiltonian is $H = H_N + V_C - H_{\text{c.m.}}$, where H_N , V_C and $H_{\text{c.m.}}$ ($= \mathbf{P}^2/2AM$ with $\mathbf{P} = \sum_i \mathbf{p}_i$) represent the nuclear Hamiltonian, the Coulomb interaction and the center-of-mass (c.m.) Hamiltonian, respectively. The nuclear Hamiltonian H_N is assumed to be

$$H_N = K + V_N; \quad K = \sum_i \frac{\mathbf{p}_i^2}{2M}, \quad V_N = \sum_{i<j} v_{ij}, \quad (1)$$

where i and j are the indices of individual nucleons. The effective interaction v_{ij} is built upon the following terms,

$$v_{ij} = v_{ij}^{(\text{C})} + v_{ij}^{(\text{LS})} + v_{ij}^{(\text{TN})} + v_{ij}^{(\text{C}\rho)} + v_{ij}^{(\text{LS}\rho)}, \quad (2)$$

with

$$\begin{aligned} v_{ij}^{(\text{C})} &= \sum_n (t_n^{(\text{SE})} P_{\text{SE}} + t_n^{(\text{TE})} P_{\text{TE}} + t_n^{(\text{SO})} P_{\text{SO}} \\ &\quad + t_n^{(\text{TO})} P_{\text{TO}}) f_n^{(\text{C})}(r_{ij}), \\ v_{ij}^{(\text{LS})} &= \sum_n (t_n^{(\text{LSE})} P_{\text{TE}} + t_n^{(\text{LSO})} P_{\text{TO}}) f_n^{(\text{LS})}(r_{ij}) \\ &\quad \cdot [\mathbf{L}_{ij} \cdot (\mathbf{s}_i + \mathbf{s}_j)], \\ v_{ij}^{(\text{TN})} &= \sum_n (t_n^{(\text{TNE})} P_{\text{TE}} + t_n^{(\text{TNO})} P_{\text{TO}}) f_n^{(\text{TN})}(r_{ij}) r_{ij}^2 S_{ij}, \\ v_{ij}^{(\text{C}\rho)} &= (C^{(\text{SE})}[\rho(\mathbf{r}_i)] P_{\text{SE}} + C^{(\text{TE})}[\rho(\mathbf{r}_i)] P_{\text{TE}}) \delta(\mathbf{r}_{ij}). \end{aligned} \quad (3)$$

Here \mathbf{s} is the spin operator, $\mathbf{r}_{ij} = \mathbf{r}_i - \mathbf{r}_j$, $\mathbf{p}_{ij} = (\mathbf{p}_i - \mathbf{p}_j)/2$, $\mathbf{L}_{ij} = \mathbf{r}_{ij} \times \mathbf{p}_{ij}$, $S_{ij} = 4 [3(\mathbf{s}_i \cdot \hat{\mathbf{r}}_{ij})(\mathbf{s}_j \cdot \hat{\mathbf{r}}_{ij}) - \mathbf{s}_i \cdot \mathbf{s}_j]$ and $\rho(\mathbf{r})$ denotes the nucleon density. P_Y denotes the projection operator on the two-particle channel Y ($Y = \text{SE}, \text{TE}, \text{SO}, \text{TO}$). The interaction $v_{ij}^{(\text{LS}\rho)}$ is used in Sec. 4, and its form will be shown there.

The Skyrme interaction [6] assumes zero-range functions $\delta(\mathbf{r}_{ij})$ or $\nabla^2 \delta(\mathbf{r}_{ij})$ for the form factor $f_n^{(\text{X})}(r)$ ($\text{X} = \text{C}, \text{LS}, \text{TN}$), generating a quasi-local form for the resultant EDF. For the Gogny interaction, $f_n^{(\text{C})}(r)$ is taken to be Gaussian $e^{-(\mu_n r)^2}$, while $f_n^{(\text{LS})}(r)$ is set to be $\nabla^2 \delta(\mathbf{r})$ and the tensor interaction $v^{(\text{TN})}$ is ignored in the widely used parameter-sets. For the M3Y-type interactions we take $f_n^{(\text{X})}(r)$ to be the Yukawa function $e^{-\mu_n r}/\mu_n r$ for all of the density-independent channels $\text{X} = \text{C}, \text{LS}, \text{TN}$. As in the Skyrme and Gogny interactions, a density-dependent contact term $v^{(\text{C}\rho)}$ is introduced, so as to reproduce the saturation properties, with $C^{(\text{Y})}[\rho] = t_\rho^{(\text{Y})} \rho^{\alpha^{(\text{Y})}}$. As mentioned earlier, $v^{(\text{TN})}$ in M3Y-P6 is identical to that in the M3Y-Paris interaction [20].

Concerning numerical calculations, the methods detailed in Ref. [22] is applied with the basis functions given in Ref. [23]. The exchange and the pairing terms of V_C are explicitly taken into account, as well as the 2-body term of $H_{\text{c.m.}}$.

3 Prediction of magic numbers

Magic numbers are manifestation of the shell structure, which is one of fundamental ingredients of the nuclear structure theory. While magic numbers near the β stability are well established, experiments using radioactive beams disclosed that magic numbers may appear and disappear far off the β stability, depending on Z and N numbers [24]. The Z - and N -dependence of the shell structure is sometimes called *shell evolution* [25]. It has been pointed out that the tensor force $v^{(\text{TN})}$ plays important roles in the shell evolution [15,26,27]. It has also been argued that ℓ -dependence of the loosely bound s.p. levels could contribute to the shell evolution [28]. The self-consistent MF approaches with M3Y-type semi-realistic interaction, which includes the realistic tensor force, are suitable for

investigating magic numbers in the wide range of the nuclear mass table going from stable to unstable nuclei. It is noted, however, that loosely bound orbitals shall be properly handled with appropriate numerical methods [22, 23, 29].

3.1 $p0d_{3/2}$ - $p1s_{1/2}$ inversion in Ca isotopes

Although the s.p. levels are difficult to be observed unambiguously even for doubly magic nuclei, because of their fragmentation due to core polarization, they could experimentally be extracted by taking averaged energies weighted by the spectroscopic factors. Although there are not many such cases, the spectroscopic factors of $p0d_{3/2}^{-1}$ and $p1s_{1/2}^{-1}$ levels on top of ^{40}Ca and ^{48}Ca are almost exhausted in experiments [30, 31]. Interestingly, the experimental results indicate an inversion of these two levels from ^{40}Ca to ^{48}Ca .

For the doubly magic nuclei ^{40}Ca and ^{48}Ca , the spherical HF is expected to give a good approximation of the ground-state wave functions. Then the $p0d_{3/2}$ and $p1s_{1/2}$ energies in the HF can be compared to the experimental energies averaged by the spectroscopic factors. Some effective interactions reproduce the $p1s_{1/2}$ - $p0d_{3/2}$ inversion, but others do not [32, 33]. However, even with the interactions that reproduce the inversion, the slope of the s.p. level spacing $\Delta\varepsilon_{13} = \varepsilon(p1s_{1/2}) - \varepsilon(p0d_{3/2})$ from ^{40}Ca to ^{48}Ca is not reproduced, except for the relativistic HF calculation with PKA1 [34].

The s.p. energies are calculated for the individual Ca isotopes within the spherical HF regime, on the equal-filling assumption when necessary. The slope is also quite well reproduced with the semi-realistic M3Y-Pn interactions as shown in Fig. 1 and in Ref [27]. Moreover, we find that the N -dependence of $\Delta\varepsilon_{13}$ is quite different from the N -dependence in the previous results without tensor force, as exemplified by the difference between the M3Y-P6 result and the result of the Gogny-D1S interaction in Fig. 1. To confirm the important role of the tensor-force, we evaluate contribution of $v^{(\text{TN})}$ to the s.p. energy as

$$\begin{aligned} \varepsilon^{(\text{TN})}(j) &= \sum_{j'm'} n_{j'} \langle jmj'm' | v^{(\text{TN})} | jmj'm' \rangle \\ &= \frac{1}{2j+1} \sum_{j'J} n_{j'} (2J+1) \langle jj'J | v^{(\text{TN})} | jj'J \rangle, \end{aligned} \quad (4)$$

where $n_{j'}$ denotes the occupation probability of the s.p. state j' . If we subtract the contribution of $v^{(\text{TN})}$ from the energy difference $\Delta\varepsilon_{13}$ with M3Y-P6, defining it as $\varepsilon^{(\text{TN})}(p1s_{1/2}) - \varepsilon^{(\text{TN})}(p0d_{3/2})$, the N -dependence of $\Delta\varepsilon_{13}$ becomes very similar to that of the D1S interaction (with a constant shift). This shift of the absolute value is attributed to the central and LS forces, which are adjusted under the presence (absence) of the tensor force in M3Y-P6 (D1S). These results confirm the importance of the tensor force, and show that the realistic tensor force is useful for describing the shell evolution. Similar conclusions could also be found in relativistic HF approaches [34].

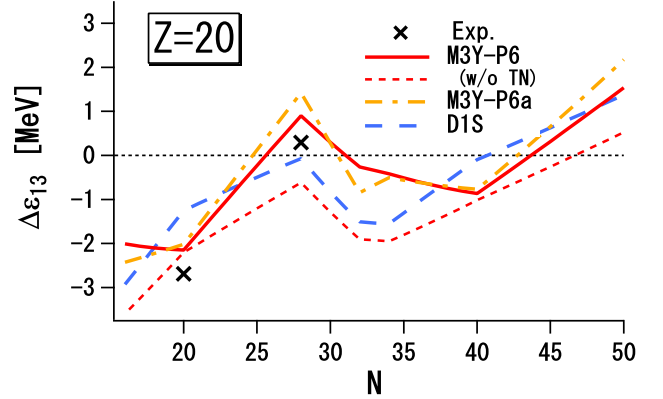


Fig. 1. $\Delta\varepsilon_{13} = \varepsilon(p1s_{1/2}) - \varepsilon(p0d_{3/2})$ for Ca isotopes. Red solid, orange dot-dashed and blue long dashed lines represent the spherical HF results with the M3Y-P6, M3Y-P6a and D1S interactions, respectively. Experimental data are obtained after average weighted by the spectroscopic factors [30, 31]. Thin red short dashed line is obtained from M3Y-P6 but by removing contribution of the tensor force (see text for more details).

$\Delta\varepsilon_{13}$ calculated with M3Y-P5', M3Y-P7 and D1M have been shown in Ref. [27]. The absolute values of $\Delta\varepsilon_{13}$ depend on the interactions to certain extent. For instance, the $p1s_{1/2}$ - $p0d_{3/2}$ inversion at ^{48}Ca is well reproduced with D1M, unlike D1S. However, N -dependence of $\Delta\varepsilon_{13}$ is primarily determined by the tensor force as pointed out above. The result of D1S nearly matches that of D1M if shifted by a constant, as in the comparison of the D1S result and the tensor-subtracted result of M3Y-P6. The same situation holds among the M3Y-Pn interactions. In Fig. 1, the result of M3Y-P6a, which is different from M3Y-P6 only in the LS channel and will be discussed in Sec. 4, is also presented. We observe that M3Y-P6a provides similar N -dependence of $\Delta\varepsilon_{13}$ to M3Y-P6, apart from the slope in $N \leq 20$ and the small staggering around $N = 32$.

3.2 Magic numbers

We have applied the M3Y-type semi-realistic interaction to prediction of magic numbers in a wide range of the nuclear mass table. From experimental viewpoints, magic numbers have been identified by the relative stability of certain nuclei with respect to masses, excitation energies, and so forth. However, there is no clear theoretical definition of magic numbers. We first discuss how magic numbers are identified in this work.

Many-body correlations are strongly quenched at magicity, because of large shell gap. Spherical HF solution is therefore expected to provide a good approximation for doubly magic nuclei, as in the case of $^{40,48}\text{Ca}$ discussed in the previous subsection. It is not easy to quantitatively compare the size of the shell gap to the strength of the many-body correlations. A rather accurate theoretical measure of the many-body correlation may however be given by pairing correlations, since it is the main

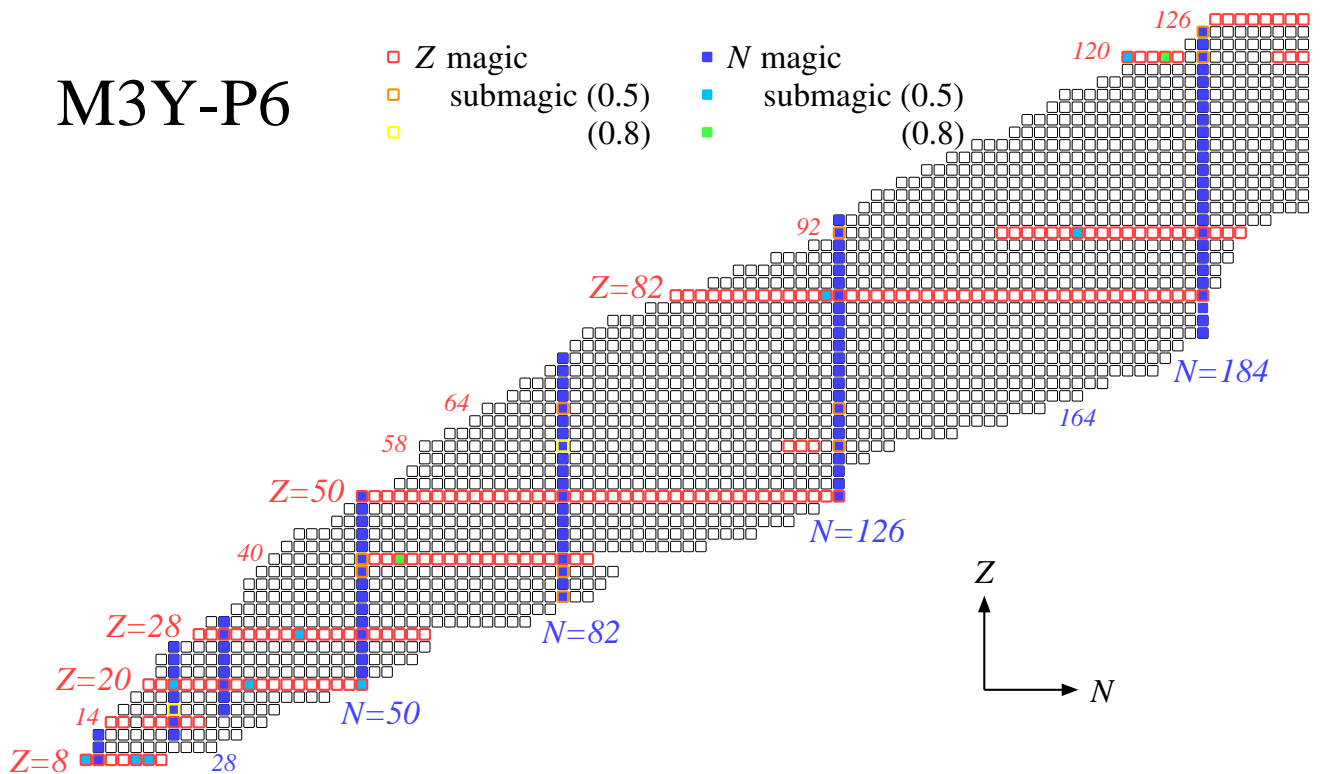


Fig. 2. Chart showing magic numbers predicted with the M3Y-P6 interaction. Individual boxes correspond to even-even nuclei. Magic (submagic) Z 's are represented by red (orange and yellow) contour of boxes, while magic (submagic) N 's by blue (skyblue and green) filled boxes. For submagic nuclei, the values for λ_{sub} are indicated in parenthesis in the caption (in MeV). Quote from Ref. [37].

correlation beyond HF in spherical nuclei. For practical identification of magic nuclei we implement spherical HFB calculations, and identify magic number in Z (N) when the proton (neutron) pair correlation vanishes. In addition, *submagic* numbers are identified if the pair correlation is quite reduced. Such suppression has been observed particularly when either Z or N is already a good magic number, drawing the counterpart to be submagic; *e.g.* $N = 40$ at ^{68}Ni [26] and $Z = 64$ at ^{146}Gd [35]. We compare the HF and the HFB energies (denoted by E_{HF} and E_{HFB}), and identify submagic Z (N) if the condensation energy $E_{\text{cond}} = E_{\text{HF}} - E_{\text{HFB}}$ is smaller than a certain value λ_{sub} for $N = \text{magic}$ ($Z = \text{magic}$) nuclei. The λ_{sub} value is rather arbitrary, and we shall show results of $\lambda_{\text{sub}} = 0.5 \text{ MeV}$ and 0.8 MeV below. Considering the domain where MF approaches are rather valid and the experimental accessibilities, we restrict our calculations to $8 \leq Z \leq 126$, $N \leq 200$.

When a nucleus is identified as not being magic, it reveals a small shell gap that could not quench many-body correlations in the present spherical HFB calculation. Quadrupole deformation, which is not considered here, could still be important in some cases. The present criterion remains however quite useful to pick up candidates for magicity. Quadrupole deformation will be investigated in future studies.

Magic and submagic numbers predicted with the M3Y-P6 interaction are shown in Fig. 2. It is noticeable that the results with M3Y-P6 are not contradictory to available experimental data except in a few cases. For instance, $N = 16$ comes submagic at ^{24}O , and so does $N = 32$ at ^{52}Ca , $N = 40$ at ^{68}Ni , $Z = 64$ at ^{146}Gd . The $N = 28$ magicity is lost in $Z \leq 14$ while kept in $Z \geq 16$. Although the disappearance of the $N = 20$ magic number is correctly reproduced for ^{30}Ne , it still is magic at ^{32}Mg in Fig. 2, which is one of the few exceptions. This disagreement with the data will probably be reduced by considering quadrupole deformation [36].

In Ref. [37], more results are presented, which are obtained from other interactions such as M3Y-P7 and D1M. Unlike for the M3Y-P6 interaction, predictions based on M3Y-P7 and D1M are much less consistent with experimental data for a large number of nuclides. A part of the success of the M3Y-P6 interaction is certainly attributed to the contribution of the realistic tensor force, although the other channels are also important as the comparison to M3Y-P7 illustrates.

To measure the effects of the tensor force on the shell gap, the double difference of the s.p. energies, $\Delta\epsilon(j_2 - j_1) = \epsilon(j_2) - \epsilon(j_1)$ at a certain nuclide (Z_b, N_b) relative to that at a reference nuclide (Z_a, N_a), is denoted by $\delta\Delta\epsilon(j_2 - j_1)$, and is calculated for the HF results with M3Y-P6. Replac-

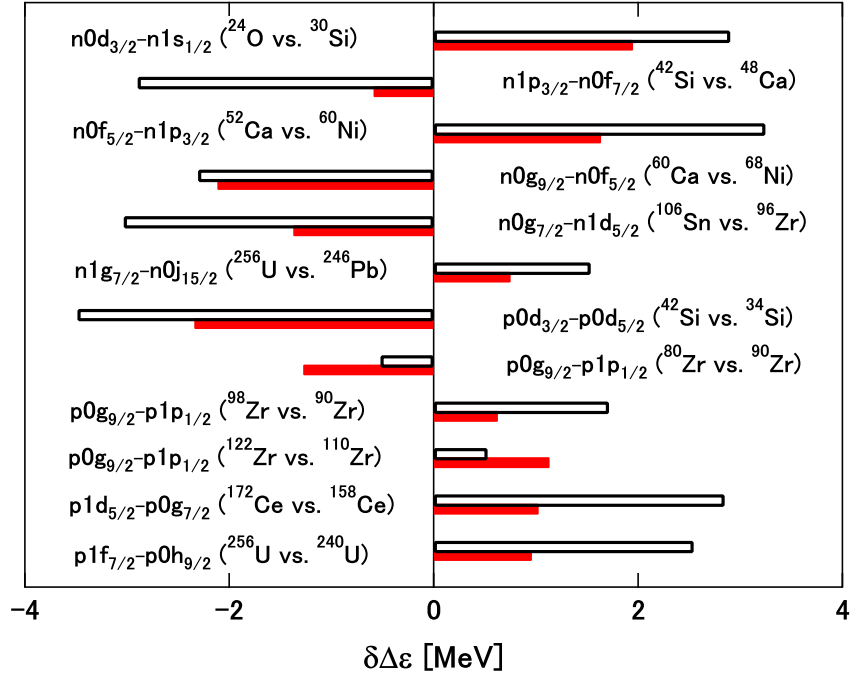


Fig. 3. Difference of the shell gaps between two members of isotopes or isotones $\delta\Delta\varepsilon(j_2 - j_1)$ (open bars), with contributions of $v^{(\text{TN})}$ (red bars) to it, obtained from the HF results with M3Y-P6.

ing $\varepsilon(j)$ by $\varepsilon^{(\text{TN})}(j)$ of Eq. (4), we also evaluate tensor-force contribution to $\delta\Delta\varepsilon(j_2 - j_1)$. Some results are presented in Fig. 3. For instance, the top row indicates that the shell gap between $n0d_{3/2}$ and $n1s_{1/2}$ increases by about 3 MeV from ³⁰Si to ²⁴O, and about 2 MeV out of 3 MeV comes from the tensor force. This tells us importance of the tensor force in the new magicity $N = 16$ around ²⁴O. Significance of the tensor force is found also in the $N = 32$ magicity at ⁵²Ca. It is interesting to notice that similar results have been obtained within a relativistic framework including Lorentz tensor coupling [34].

4 Isotope shifts for nuclei with magic proton numbers

Accurate measurements of isotope shifts [38, 39] have questioned the predictivity of nuclear structure theories for a long period. One is the conspicuous kink at $N = 126$ in the neutron-rich Pb isotope. Although the kink itself can be reproduced in a relativistic MF approach [40] and in a non-relativistic approach with the modified Skyrme EDF [41], in those results the s.p. level spacing between $n1g_{9/2}$ and $n0i_{11/2}$ is found to be too small. Another long-standing challenge for the MF theories is the reproduction of the very close charge radii between ⁴⁰Ca and ⁴⁸Ca. Both of these two nuclei are doubly magic and hence expected to be well described by MF theories. However, to our best knowledge, no self-consistent calculations have been able to reproduce their close charge radii so far.

As shown below, these deficiencies are related to the LS interaction. While the ℓs splitting plays an essential role

in the nuclear shell structure, it has been difficult so far to account for the observed size of the ℓs splitting only from the $2N$ interaction [42]. Recently, Kohno has pointed out, based on the chiral effective-field theory (χ EFT), that the $3N$ LS interaction may account for the missing part of the ℓs splitting [43, 44]. In the following, we explore this idea and incorporate the $3N$ LS interaction in our MF model, reinvestigating the issue of the isotope shifts of the nuclei with magic proton numbers.

As shown in the previous section, the M3Y-P6 interaction gives reasonable shell structure. However, $v^{(\text{LS})}$ in M3Y-P6 is not realistic, since it is obtained phenomenologically by multiplying $v^{(\text{LS})}$ of the M3Y-Paris interaction by an overall factor of about 2 (2.2, to be precise). Here we modify the LS channel of the M3Y-P6 interaction by adding the $3N$ LS interaction suggested by Kohno, instead of enhancing $v^{(\text{LS})}$. In practice we use a density-dependent LS interaction $v^{(\text{LS}\rho)}$, which is defined as

$$v_{ij}^{(\text{LS}\rho)} = 2i D[\rho(\mathbf{R}_{ij})] \mathbf{p}_{ij} \times \delta(\mathbf{r}_{ij}) \mathbf{p}_{ij} \cdot (\mathbf{s}_i + \mathbf{s}_j), \quad (5)$$

where $\mathbf{R}_{ij} = (\mathbf{r}_i + \mathbf{r}_j)/2$. Because the $3N$ LS interaction is short range, effects of the third nucleon are well approximated by a linear function of ρ for the coefficient $D[\rho]$. The functional form of $D[\rho]$ is therefore taken to be

$$D[\rho(\mathbf{r})] = -w_1 \frac{\rho(\mathbf{r})}{1 + d_1 \rho(\mathbf{r})}. \quad (6)$$

The d_1 term in the denominator suppresses instability in the MF towards extremely high densities. We adopt $d_1 = 1.0 \text{ fm}^3$, after confirming that the results of the MF calculations are insensitive to d_1 . The parameter w_1 is

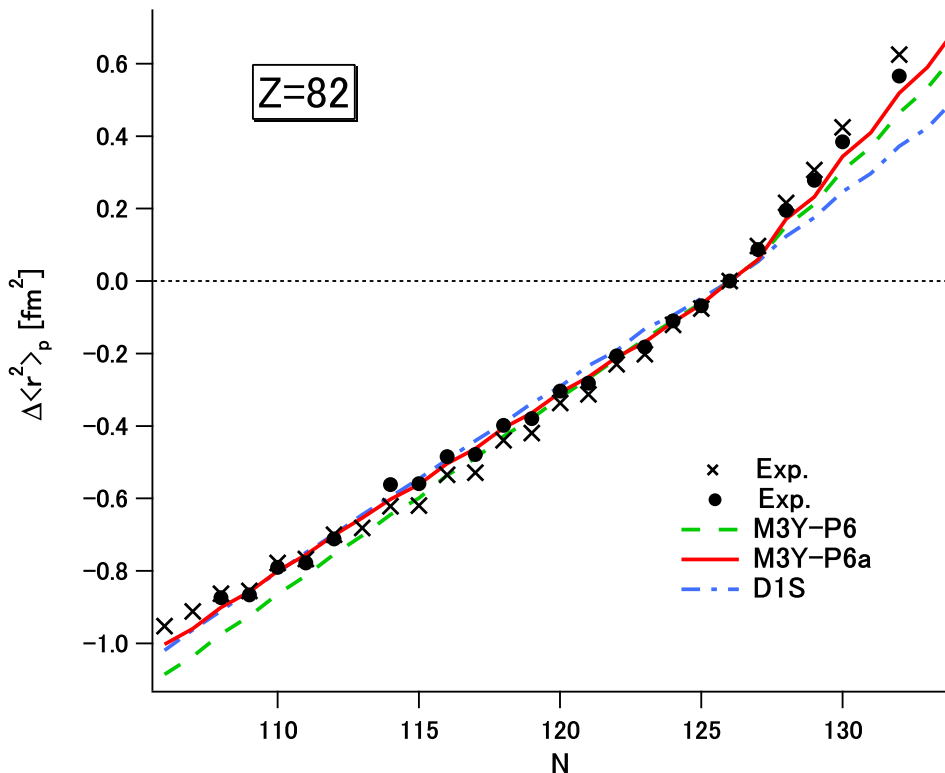


Fig. 4. Isotope shifts of the Pb nuclei $\Delta\langle r^2 \rangle_p(^A\text{Pb})$, obtained from the HFB calculations with M3Y-P6a (red solid line), in comparison to those with M3Y-P6 (green dashed line) and D1S (blue dot-dashed line). Experimental data are quoted from Refs. [45] (crosses) and [38] (circles).

fixed so as to reproduce the $n0i_{13/2}$ - $n0i_{11/2}$ splitting with M3Y-P6 at ^{208}Pb . This new interaction is called M3Y-P6a. Except for the LS interaction, the other terms of M3Y-P6a are identical to the original M3Y-P6 interaction.

The coefficient $D[\rho]$ in $v^{(\text{LS}\rho)}$ increases as the density grows, and makes the ls potential stronger (weaker) in the nuclear interior (exterior). Therefore the s.p. function of the $j = \ell + 1/2$ ($j = \ell - 1/2$) orbit tends to shift inward (outward), as has been confirmed in Fig. 1 of Ref. [21]. This mechanism gives a certain improvement in the isotope shifts of the Pb nuclei. It also plays a crucial role in reproducing the close charge radii between ^{40}Ca and ^{48}Ca . We shall illustrate these by the spherical HFB calculations with M3Y-P6a, in comparison with those with M3Y-P6. The spherical HFB results with D1S are also presented. Together with M3Y-P6, the D1S interaction will show the general trend that is given by conventional interactions without the $3N$ LS term.

4.1 Pb isotopes

In the Pb nuclei, it is customary to define the isotope shifts by taking ^{208}Pb as a reference, $\Delta\langle r^2 \rangle_p(^A\text{Pb}) = \langle r^2 \rangle_p(^A\text{Pb}) - \langle r^2 \rangle_p(^{208}\text{Pb})$. We depict $\Delta\langle r^2 \rangle_p(^A\text{Pb})$ in Fig. 4, comparing the HFB results with M3Y-P6a (red solid line) to those with M3Y-P6 (green dashed line).

The lowest neutron s.p. level beyond $N = 126$ is $n1g_{9/2}$ [46]. It is known that the partial $n0i_{11/2}$ occupation due to the pair correlation increases the slope of the isotope shift $\Delta\langle r^2 \rangle_p(^A\text{Pb})$ at $N > 126$. Therefore the s.p. spacing between $n1g_{9/2}$ and $n0i_{11/2}$ is a quantity significant to the kink. This s.p. spacing is largely influenced by the isospin content of the LS interaction [40,41]. However, the reproduction of the kink only from the $2N$ LS interaction requires that the $n1g_{9/2}$ and $n0i_{11/2}$ levels are almost degenerate, or even inverted [47]. This is in contradiction with the experimental data of the s.p. levels extracted from the low-lying states of ^{209}Pb [46]. When the $3N$ LS interaction (or ρ -dependent LS interaction) is considered, the mean radius of $n0i_{11/2}$ increases and produces a stronger kink at $N = 126$ as long as $n0i_{11/2}$ is populated to certain degree. This effect of the $3N$ LS interaction on the isotope shifts is confirmed by comparing the M3Y-P6a results to those of M3Y-P6. With M3Y-P6a, we have $\varepsilon(n0i_{11/2}) - \varepsilon(n1g_{9/2}) = 0.72$ MeV at ^{208}Pb , close to the observed energy difference between $9/2^+$ and $11/2^+$ at ^{209}Pb (0.78 MeV). We shall mention that the kink at $N = 126$ is nevertheless reproduced, comparably well to the models presented in Refs. [40,41].

It is remarked that both $v^{(\text{LS})}$ and $v^{(\text{LS}\rho)}$ are equally important for the description of the kink. $v^{(\text{LS})}$ is realistic and has reasonable isospin content, giving appropriate s.p. spacing between $n1g_{9/2}$ and $n0i_{11/2}$. If the s.p. spacing is

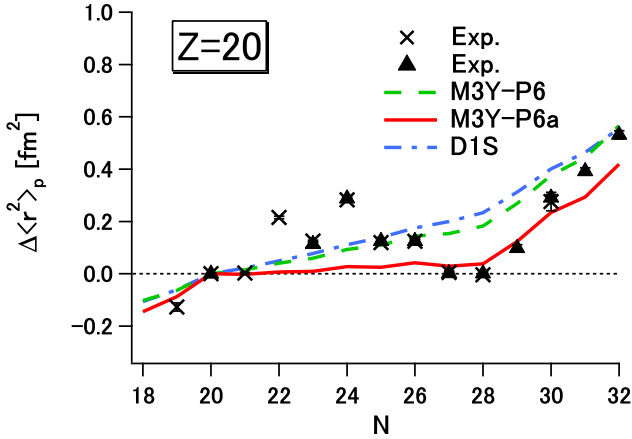


Fig. 5. Isotope shifts of the Ca nuclei $\Delta\langle r^2 \rangle_p(^A\text{Ca})$. Experimental data are taken from Ref. [50] (triangles) as well as from [45] (crosses). See Fig. 4 for other conventions.

too large as it is the case with most Skyrme and Gogny interactions that have a contact LS force, pair excitations to $n0i_{11/2}$ are negligible and the slope beyond $N > 126$ is not described well, even if $v^{(LS\rho)}$ is introduced and the s.p. function of $n0i_{11/2}$ distribute broadly.

In Ref. [48], the generator-coordinate method was applied to the isotope shifts of the Pb nuclei, by using the SLy4 parameter-set of the Skyrme interaction. While influence of correlations beyond the MF approximations was observed in light Pb nuclei with $100 \lesssim N \lesssim 115$, related to the shape coexistence in this region, it was found that the kink at $N = 126$ could hardly be reproduced.

Let us stress that the LS part of M3Y-P6a ($v^{(LS)} + v^{(LS\rho)}$) is almost realistic, since it is comprised of the $2N$ LS part of the M3Y-Paris interaction and the $3N$ interaction suggested by the microscopic χ EFT. The w_1 parameter is, however, still a free parameter, not well determined from the χ EFT. This is mostly because the χ EFT is not yet a convergent framework. Still, it is emphasized that the χ EFT provides an important extension of the LS interaction, which gives a qualitative improvement for the description of isotope shifts in Pb.

4.2 Ca isotopes

By taking ^{40}Ca as a reference, the isotope shifts of the Ca nuclei are defined by $\Delta\langle r^2 \rangle_p(^A\text{Ca}) = \langle r^2 \rangle_p(^A\text{Ca}) - \langle r^2 \rangle_p(^{40}\text{Ca})$. The HFB results are depicted in Fig. 5, in comparison with the experimental data.

If the $3N$ LS interaction is taken into account, the $n0f_{7/2}$ function shifts inward, which reduces the radius of ^{48}Ca . Because of this effect, we have $\Delta\langle r^2 \rangle_p(^{48}\text{Ca}) \approx 0$, i.e. $\langle r^2 \rangle_p(^{40}\text{Ca}) \approx \langle r^2 \rangle_p(^{48}\text{Ca})$, in the M3Y-P6a result. Thus the close radii between ^{40}Ca and ^{48}Ca are well described in the self-consistent calculation for the first time. More detailed analysis is given in Ref. [49].

Very recently it is reported [50] that *ab initio* calculations with the χ EFT $2N + 3N$ interaction reproduce the

close radii between ^{40}Ca and ^{48}Ca , by using the coupled-cluster and the similarity-renormalization-group methods. Consistent with these *ab initio* results, the present MF results with the semi-realistic interaction seem to clarify what is key to solve this long-standing problem and that it is closely linked to the other problems; the origin of the ls splitting and the kink in the isotope shifts of the Pb nuclei.

Having sizable deviation from those of $^{40,48}\text{Ca}$, the experimental isotope shifts of $^{42-46}\text{Ca}$ are not described by the spherical HFB calculation. This discrepancy will be ascribed to effects beyond MF, which may include excitations out of the ^{40}Ca core [51].

4.3 Sn isotopes

We next present the isotope shifts of the Sn nuclei in Fig. 6, $\Delta\langle r^2 \rangle_p(^A\text{Sn}) = \langle r^2 \rangle_p(^A\text{Sn}) - \langle r^2 \rangle_p(^{120}\text{Sn})$, by adopting ^{120}Sn as a reference.

The spherical HFB calculations with M3Y-P6a reproduce $\Delta\langle r^2 \rangle_p(^A\text{Sn})$ in a long chain of the Sn isotopes. In particular, the curve in $70 < N < 82$ is in good agreement with the data, in which the occupation of $n0h_{11/2}$ plays a significant role. Since the $3N$ LS interaction shrinks the s.p. function of $n0h_{11/2}$, the slope of $\Delta\langle r^2 \rangle_p(^A\text{Sn})$ comes less steep in $70 < N < 82$. Moreover, we predict a kink at $N = 82$ in the M3Y-P6a result. This takes place due to the pair excitation to $n0h_{9/2}$, similarly to the kink at $N = 126$ in the Pb nuclei. Such a kink is not observed in the results without the $3N$ LS interaction, even if correlations beyond MF are taken into account [48]. Thus it is generally expected that the $3N$ LS interaction tends to give a kink in the isotope shifts, or to make a kink stronger, at the neutron jj -closed shell. Measurements of $\Delta\langle r^2 \rangle_p(^A\text{Sn})$ beyond $N = 82$ are of great interest, which may confirm the $3N$ LS effects further.

5 Conclusion

The M3Y-type semi-realistic interaction has been applied to the self-consistent MF calculations under the spherical symmetry. Particular focus is placed on roles of the non-central forces, for which we refer to the realistic interaction. The non-central forces on a realistic bases is significant to describe nuclear shell structure reasonably well. This seems to resonate Gogny's original idea to determine effective central force. Several examples have been presented: (i) $p0d_{3/2}$ - $p1s_{1/2}$ inversion in Ca isotopes, to which the realistic tensor force gives correct N -dependence, (ii) prediction of magic numbers in a wide range of the mass table, to which the M3Y-P6 interaction gives results compatible with almost all available data with a few exceptions, (iii) isotope shifts of $Z = \text{magic}$ nuclei, the kink at $N = 126$ in Pb and close radii of $^{40,48}\text{Ca}$ in particular, which are greatly improved by the $3N$ LS interaction indicated by the χ EFT, in addition to the realistic $2N$ LS interaction. It is now clear that realistic interaction is definitely useful for nuclear mean-field approaches, and

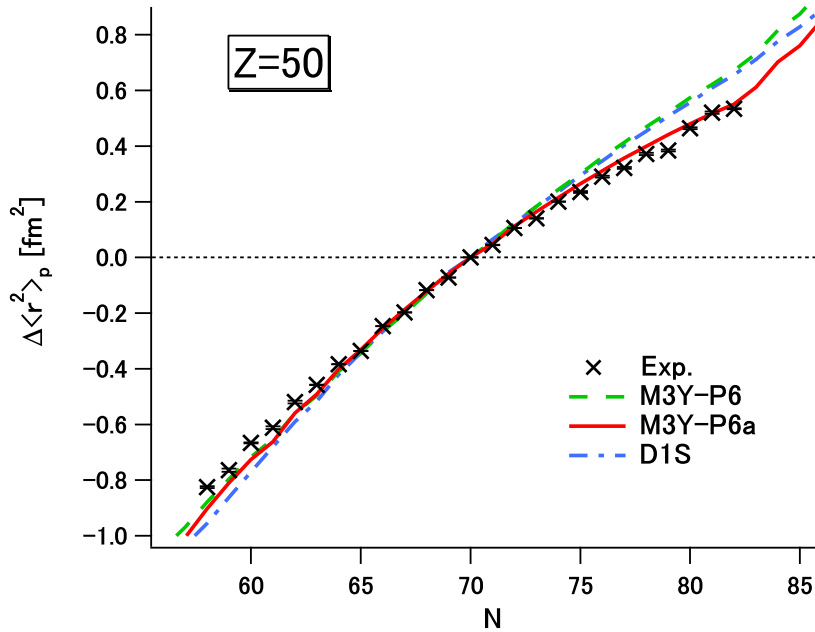


Fig. 6. Isotope shifts of the Sn nuclei $\Delta\langle r^2 \rangle_p(^A\text{Sn})$. See Fig. 4 for conventions.

besides, semi-realistic interactions may bridge the gap between *ab initio* calculations and MF (or EDF) approaches.

Acknowledgments

This work is financially supported in part by JSPS KAKENHI Grant Number 24105008 and Grant Number 16K05342

References

1. P. Ring and P. Schuck, *The Nuclear Many-Body Problem* (Springer, New York, 1980), Chapt. 5 and 7.
2. D. Vautherin and D.M. Brink, *Phys. Rev. C* **5** (1972) 626.
3. M. Beiner, H. Flocard, N. van Giai and P. Quentin, *Nucl. Phys. A* **238** (1975) 29.
4. D. Gogny, *Nuclear Self-Consistent Fields*, edited by G. Ripka and M. Porneuf (North-Holland, Amsterdam, 1975), p. 333.
5. J. Dechargé and D. Gogny, *Phys. Rev. C* **21** (1980) 1568.
6. T.H.R. Skyrme, *Phil. Mag.* **1** (1956) 1043.
7. T.H.R. Skyrme, *Nucl. Phys.* **9** (1959) 615.
8. J. Dobaczewski, H. Flocard and J. Treiner, *Nucl. Phys. A* **422** (1984) 103.
9. P. Ring and P. Schuck, *The Nuclear Many-Body Problem* (Springer, New York, 1980), Chapt. 4.
10. J.F. Berger, M. Girod and D. Gogny, *Comp. Phys. Comm.* **63** (1991) 365.
11. S. Goriely, S. Hilaire, M. Girod and S. Pèru, *Phys. Rev. Lett.* **102** (2009) 242501.
12. T. Otsuka, T. Matsuo and D. Abe, *Phys. Rev. Lett.* **97** (2006) 162501.
13. M. Anguiano, G. Co', V. De Donno and A.M. Lallena, *Phys. Rev. C* **83** (2011) 064306.
14. G. Co', V. De Donno, M. Anguiano and A.M. Lallena, *ibid.* **85** (2012) 034323. M. Anguiano, M. Grasso, G. Co', V. De Donno and A.M. Lallena, *ibid.* **86** (2012) 054302.
15. T. Otsuka, T. Suzuki, R. Fujimoto, H. Grawe and Y. Akaishi, *Phys. Rev. Lett.* **95** (2005) 232502.
16. H. Sagawa and G. Colò, *Prog. Part. Nucl. Phys.* **76** (2014) 76.
17. H. Nakada, *Phys. Rev. C* **68** (2003) 014316.
18. H. Nakada, *Phys. Rev. C* **87** (2013) 014336.
19. G. Bertsch, J. Borysowicz, H. McManus and W.G. Love, *Nucl. Phys. A* **284** (1977) 399.
20. N. Anantaraman, H. Toki and G.F. Bertsch, *Nucl. Phys. A* **398** (1983) 269.
21. H. Nakada and T. Inakura, *Phys. Rev. C* **91** (2015) 021302(R).
22. H. Nakada, *Nucl. Phys. A* **764** (2006) 117; *ibid.* **801** (2008) 169.
23. H. Nakada, *Nucl. Phys. A* **808** (2008) 47.
24. O. Sorlin and M.-G. Porquet, *Prog. Part. Nucl. Phys.* **61** (2008) 602.
25. T. Otsuka, *Eur. Phys. J ST* **156** (2008) 169.
26. H. Nakada, *Phys. Rev. C* **81** (2010) 051302(R).
27. H. Nakada, K. Sugiura and J. Margueron, *Phys. Rev. C* **87** (2013) 067305.
28. A. Ozawa *et al.*, *Phys. Rev. Lett.* **84** (2000) 5493.
29. H. Nakada and M. Sato, *Nucl. Phys. A* **699** (2002) 511; *ibid.* **714** (2003) 696.
30. P. Doll, G.J. Wagner, K.T. Knöpfle and G. Mairle, *Nucl. Phys. A* **263** (1976) 210.
31. C.A. Ogilvie *et al.*, *Nucl. Phys. A* **465** (1987) 445.
32. M. Grasso, Z.Y. Ma, E. Khan, J. Margueron and N. Van Giai, *Phys. Rev. C* **76** (2007) 044319.
33. Y.Z. Wang, J.Z. Gu, X.Z. Zhang and J.M. Dong, *Phys. Rev. C* **84** (2011) 044333.
34. Jiajie Li, J. Margueron, W.H. Long and N. Van Giai, *Phys. Lett. B* **753** (2015) 97.

35. T. Matsuzawa, H. Nakada, K. Ogawa and G. Momoki, Phys. Rev. C **62** (2000) 054304; *ibid.* **63** (2001) 029902(E).
36. Y. Suzuki, H. Nakada and S. Miyahara, submitted to Phys. Rev. C (e-Print arXiv: 1604:03202 [nucl-th]).
37. H. Nakada and K. Sugiura, Prog. Theor. Exp. Phys. (2014) 033D02.
38. P. Aufmuth, K. Heilig and A. Steudel, At. Data Nucl. Data Tables **37** (1987) 455.
39. I. Angeli, At. Data Nucl. Data Tables **87** (2004) 185.
40. M.M. Sharma, G. Lalazissis and P. Ring, Phys. Lett. B **317** (1994) 9.
41. P.-G. Reinhard and H. Flocard, Nucl. Phys. A **584** (1995) 467.
42. K. Andō and H. Bandō, Prog. Theor. Phys. **66** (1981) 227.
43. M. Kohno, Phys. Rev. C **86** (2012) 061301(R).
44. M. Kohno, Phys. Rev. C **88** (2013) 064005.
45. I. Angeli and K.P. Marinova, At. Data Nucl. Data Tables **99** (2013) 69.
46. R.B. Firestone *et al.*, *Table of Isotopes*, 8th edition (John Wiley & Sons, New York, 1996).
47. P.M. Goddard, P.D. Stevenson and A. Rios, Phys. Rev. Lett. **110** (2013) 032503.
48. M. Bender, G.F. Bertsch and P.-H. Heenen, Phys. Rev. C **73** (2006) 034322.
49. H. Nakada, Phys. Rev. C **92** (2015) 044307.
50. R.F. Garcia Ruiz *et al.*, Nat. Phys. **12** (2016) 594.
51. E. Caurier, K. Langanke, G. Martínez-Pinedo, F. Nowacki and P. Vogel, Phys. Lett. B **522** (2001) 240.